Simulated Sunlight Action Spectra for Inactivation of MS2 and PRD1 Bacteriophages in Clear Water

ARTICLE *in* ENVIRONMENTAL SCIENCE & TECHNOLOGY · SEPTEMBER 2011

Impact Factor: 5.33 · DOI: 10.1021/es201875x · Source: PubMed

4 AUTHORS:

Michael B. Fisher
University of North Carolina at Chapel Hill
12 PUBLICATIONS **126** CITATIONS
SEE PROFILE

David C. Love
Johns Hopkins University
63 PUBLICATIONS **624** CITATIONS
SEE PROFILE

Rudi Schuech
University of Lincoln
5 PUBLICATIONS **23** CITATIONS
SEE PROFILE

Kara L Nelson
University of California, Berkeley
83 PUBLICATIONS **1,495** CITATIONS
SEE PROFILE

Environmental Science & Technology

ARTICLE

pubs.acs.org/est

Simulated Sunlight Action Spectra for Inactivation of MS2 and PRD1 Bacteriophages in Clear Water

Michael B. Fisher,[†] David C. Love,[†,‡] Rudi Schuech, and Kara L. Nelson*

Department of Civil and Environmental Engineering, University of California Berkeley, Berkeley, California 94720-1710, United States

Supporting Information

ABSTRACT: Action spectra for simulated sunlight were measured in clear water for two viruses: PRD1, a double-stranded DNA bacteriophage, and MS2, a single-stranded RNA bacteriophage. Viruses were diluted into phosphate buffered saline (20 mM PBS, pH 7.5) and exposed for 22 h to simulated sunlight either directly or through one of six glass filters with 50% cutoff wavelengths ranging from 280 to 350 nm. Virus survival was measured using the double agar layer plaque method. Both UVA (320−400 nm) and UVB (280−320 nm) light were found to contribute to PRD1 inactivation, while only UVB inactivated MS2. A computational model was developed for interpreting these action spectra with 3-nm resolution. Using these methods, we provide detailed estimates of the sensitivity of MS2 and PRD1 to photoinactivation from 285 to 345 nm. The resulting sensitivity coefficients can be combined with solar spectra to estimate inactivation rates in clear water under different sunlight conditions. This approach will be useful for modeling the inactivation of viruses and other microorganisms in sunlit natural and engineered systems.

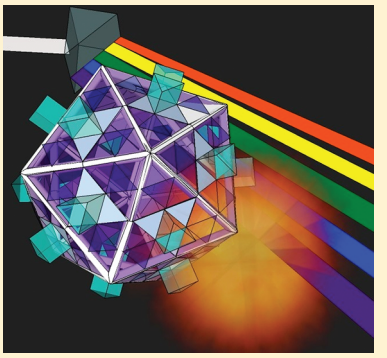

INTRODUCTION

The germicidal properties of natural sunlight and artificial light on animal viruses,[1] plant viruses,[2] bacterial viruses (bacteriophage),[3] bacteria,[3] and fungi[4] are longstanding research topics. The biological response (i.e., persistence, inactivation, mutation) of an organism to ultraviolet (UV) light exposure over a range of wavelengths can be described by photoaction spectra[3,5] and biological weighting functions.[6] The earliest action spectra were obtained primarily in order to characterize the chemical and biological structures of microorganisms;[7] researchers first determined that genes were composed of nucleic acids when action spectra for mutations in corn pollen, fungi, and viruses matched nucleic acid absorbance spectra.[8−10] Because one of the absorption maxima of DNA occurs near 260 nm[11] and because of the technical limitations of the light sources traditionally used, most action spectra studies have only utilized wavelengths spanning a portion of the UVC region (190−280 nm). Action spectra (or BWFs) for solar UV wavelengths have been determined to quantify the effects of ozone depletion on biological processes, particularly photosynthesis.[5,6] These functions were designed to quantify the impacts of changes in irradiance spectra on the relative rates of biological processes, rather than to predict or model the absolute rates of these processes.

Understanding the role of sunlight in inactivating viruses and other microorganisms requires characterizing the effects of the different solar wavelengths that reach the surface of the earth, especially in the UVB (280−320 nm) and UVA (320−400 nm) regions. While action spectra for the loss of culturability of many organisms closely correspond to the absorption spectra of their genetic material in the UVC region, photoaction spectra for sunlight inactivation in the UVB and UVA regions may be quite different.[11,12] Longer wavelengths may damage organisms through a variety of mechanisms including protein damage[13,14] and reactions with endogenous and exogenous sensitizers to form potentially harmful reactive oxygen species (ROS).[15] Few studies have produced UVB and UVA action spectra for viruses.[16−18] In addition, out of all the previous studies of natural and simulated sunlight inactivation of viruses, only those of Sinton and colleagues[19,20] measured and reported the spectrum of the light used, which is critical information for interpreting results.

In this study we developed action spectra for one DNA and one RNA virus in clear water (no exogenous sensitizers) using polychromatic simulated sunlight. We modeled the viruses' response to simulated sunlight to develop coefficients for estimating the sensitivity of each virus to wavelengths over the 280−496 nm range with 3-nm resolution. These spectral sensitivity coefficients can be combined with measured or predicted sunlight intensity spectra to estimate inactivation rates under different sunlight conditions.

MATERIALS AND METHODS

Viruses. MS2, a single stranded 3.6-kbp RNA bacteriophage, and PRD1, a double stranded 15-kbp DNA bacteriophage, were propagated in *E. coli* F_{amp} (ATCC no. 700891) and in

Received: June 1, 2011
Accepted: September 21, 2011
Revised: September 13, 2011
Published: September 21, 2011

Table 1. Linear Regression Coefficients for MS2 and PRD1 for Each of Eight Simulated Sunlight Exposure Conditions

filter	MS2 (n = 3)			PRD1 (n = 3)		
	sig dif[a]	k_{obs} (h^{-1}) ± stdev	R^2 ± stdev	sig dif	k_{obs} (h^{-1}) ± stdev	R^2 ± stdev
no filter	A	0.148 ± 0.004	0.985 ± 0.005	A	0.475 ± 0.043	0.986 ± 0.013
f-280[b]	B	0.107 ± 0.009	0.986 ± 0.011	B	0.407 ± 0.007	0.996 ± 0.001
f-295	C	0.076 ± 0.005	0.979 ± 0.021	B	0.374 ± 0.041	0.992 ± 0.002
f-305	D	0.060 ± 0.003	0.856 ± 0.121	B	0.338 ± 0.038	0.997 ± 0.003
f-320	E	0.009 ± 0.004	0.489 ± 0.136	C	0.199 ± 0.025	0.997 ± 0.002
f-335	E	0.013 ± 0.006	0.808 ± 0.105	C/D[c]	0.159 ± 0.005	0.995 ± 0.003
f-345	E	0.005 ± 0.002	0.983 ± 0.022	D	0.107 ± 0.008	0.983 ± 0.022
Dark	E	0.003 ± 0.001	0.634 ± 0.049	E	0.002 ± 0.005	0.429 ± 0.859

[a] $p < 0.05$. [b] $n = 2$ for f-280 for MS2 and PRD1. [c] PRD1 inactivation with a WG320 filter was similar to the f-335 filter but different than f-345 filter, while the PRD1 inactivation rates with f-335 and f-345 filters were not different from each other.

Salmonellatyphimurium LT2 (ATCC no. 19585), respectively, by broth enrichment.[21] Bacteriophage and hosts were kindly provided by Prof. Mark Sobsey (University of North Carolina). Bacteriophage enrichments were purified as described in the Supporting Information (SI). Previous research suggests that these methods adequately remove broth photosensitizers capable of contributing to indirect inactivation of the phage.[22]

Bacteriophage plaque assays were performed using the double agar layer (DAL) method[23] to titer stocks and to enumerate viruses after exposure to UV light as described in the SI.

Action Spectrum Experimental Design. Purified MS2 and PRD1 were diluted together to titers of 10^6 PFU/mL in 100 mL phosphate buffered saline (PBS, 20 mM, pH 7.5) in 55 × 100 mm black-painted glass beakers ("reactors"). Samples were stirred magnetically and maintained at 20 °C in a water bath with a recirculating chiller (Thermo Electron). Sample beakers were (i) left uncovered; (ii) covered with 5 × 5 cm square glass optical cutoff filters [glass filters: Schott WG280 ("f-280"), Schott WG295 ("f-295"), Schott WG305 ("f-305"), Schott WG320 ("f-320"), Schott KG5 ("f-335"), and Kopp 9345 ("f-345")]; or (iii) covered with aluminum foil for dark controls and exposed to simulated sunlight for 22 h. Subsamples were removed at 0, 2, 4, 6, 8, 12, 22 h and immediately frozen at −80 °C. Experiments were performed in triplicate over three consecutive days (each condition was tested in one reactor each day). The measured biological response to simulated sunlight was loss of culturability (ability to form plaques), which was quantified as described above.

Glass filters had 50% transmittance values at wavelengths ranging from 280 to 350 nm (SI Figure S1 A). Filter transmittance spectra were recorded on a Perkin-Elmer Lambda 14 UV−visible spectrophotometer (Waltham, MA), and lamp intensity spectra were adjusted for the absorbance of each filter as described in the SI.

Solar Simulator. Samples were irradiated using an ozone-free 1000 W Xe arc lamp housed in an Oriel solar simulator (Oriel model # 91194−1000, Newport Co., Irvine, CA) which was fitted with an Oriel AM 1.5:G:A "global" filter and an atmospheric attenuation filter (Oriel part no. 81017, Newport Co.) to simulate a solar spectrum (SI Figure S1 B, no filter). Spectra were measured using calibrated portable UV−visible spectroradiometers (RPS 200 and RPS 380, International Light, Peabody, MA). Both the simulator configuration and spectral measurements are described in greater detail in the SI. Solar simulator output over the course of the experiments was constant at 277 W/m^2 summed over 280−700 nm.

Model Development. *Intensity Spectra.* Each of the seven reactors was covered with a different filter (or none), and thus delivered a different light spectrum. The transmittance of each filter multiplied by the solar simulator irradiance at each wavelength is shown in SI Figure S1 B (the raw irradiance data are used for the no filter condition). These spectra represent the intensity to which organisms in the different reactors were exposed and were used as inputs for the numerical model.

Inactivation curves. Virus inactivation was modeled using pseudo first-order kinetics (see below); inactivation rate constants (k^i_j) were calculated as the negative slope of the linear regression lines ($\ln(N/N_o)$ vs time) for each combination of virus (i) and reactor (j).These kinetics were found to accurately describe the measured data (Table 1).

Inactivation Model. Inactivation rate constants were modeled using eq 1:

$$k^i_j = \int_0^\infty [I_j(\lambda) \times P^i(\lambda)]d\lambda \quad (1)$$

Where $I_j(\lambda)$ is the spectral irradiance of light (in $W/m^2 \cdot nm$) delivered to reactor j and $P^i(\lambda)$ is the spectral sensitivity coefficient, or the relative contribution (in $m^2/W \cdot h$) of photons at wavelength λ to the inactivation rate of organism i. Because measurements revealed that the solution absorbed less than 1% of light at all wavelengths of interest, and the reflection factor, divergence factor, and Petri factor[24] were each found to differ from 1 by less than 5%, the simplifying assumption $I(\lambda) = I_0(\lambda)$ could be made.

To further simplify calculations, spectra were discretized into 3 nm bins (chosen to provide sufficient resolution without requiring excessive computing time). Thus, $I_{j,w}(\lambda)$ is the irradiance of light (in W/m^2) entering reactor j integrated over a 3 nm wavelength range centered at λ, and $P^i_w(\lambda)$ is the average spectral sensitivity coefficient, or the relative contribution (in $m^2/W \cdot h$) of irradiance in this range to the inactivation rate of organism i. Equation 1 thus becomes:

$$k^i_j = \sum_{\lambda_{lower}}^{\lambda_{upper}} [I_{j,w}(\lambda) \times P^i_w(\lambda) \times \Delta\lambda] \quad (2)$$

This equation is analogous to a biological weighting function (BWF) as described by Cullen and Neale.[6] An important difference is that eq 2 specifies a first-order rate constant with units of inverse time, which can be used to model the inactivation rate of viruses in sunlit waters. In contrast, the ratio of biologically

effective to measured radiation described by previous studies[5,6] is a relative measure, which is only useful if the reference condition is known.

Computational Model. A computational model was developed in MATLAB (The MathWorks, Natick, MA) to characterize action spectra by calculating the spectral sensitivity coefficients $P^i_w(\lambda)$ that best fit the measured inactivation rate constants k^i_j (which represented the mean of triplicate inactivation trials) for each virus (i) in each of the seven reactors (j). The model was run 1000 times for each virus using random initial $P^i_w(\lambda)$ guesses and the results were analyzed to obtain a single best-fit set of sensitivity coefficients $[P^i_w(\lambda)]$ for the vector of central bin wavelengths (λ) for each organism (i). Briefly, the random initial $P^i_w(\lambda)$ values were iteratively adjusted using a constrained nonlinear multivariable optimization function to minimize the sum of squared errors between observed and calculated k^i_j values. Model development is described in detail and the MATLAB code is presented in the SI. Several previous studies have produced action spectra by assuming the shape can be described by an exponential or polynomial function.[5,6] We chose not to restrict the shape to avoid potentially inaccurate assumptions about the phenomena of interest. An alternative computational method that avoids such assumptions is principle component analysis (PCA).[6] We opted for an alternate optimization method designed to be less computationally intensive and facilitate multiple replicate simulations in a short period of time.

Sensitivity Analysis. Several methods were employed to characterize the sensitivity of the model output to initial conditions and measured values. For each k^i_j, alternative values were randomly chosen from within one standard deviation of that mean k^i_j value. These alternative k^i_j' values were used in the computational model to generate 100 sets of alternative spectral sensitivity coefficients, and the median and mean average deviation of these results were plotted. Sensitivity analysis procedures are described in detail in the SI.

Back-Testing. The computational approach was back-tested by generating 31 hypothetical sets of spectral sensitivity coefficients, each with a single peak centered at 250, 260, 270,...,550 nm. These hypothetical values were then used to calculate k^i_j values using eq 1. These k^i_j values were inserted into the computational model, which was solved 100 times using random initial values for P^i_w. The resulting "best fit datum" set of spectral sensitivity coefficients was compared to the hypothetical initial values to give an indication of the computational model's useful working range with the given filter set and simulated sunlight spectrum. The errors obtained for these fits were plotted as a function of peak center wavelength. The relative standard deviations of light spectrum intensities across the 7 filter conditions were also plotted in the same figure, since increased variation in light conditions was expected to contribute to improved model resolution. Additionally, a 3-peak back-test was also conducted to determine whether multiple peaks disproportionately confounded the computational model. The effects of varying the distance between peaks and the location of the three-peak ensemble were studied. Finally, a back-test was conducted using a monotonically decreasing curve to assess the performance of the model in the absence of any input peaks.

Photodamage Spectra. The spectral sensitivity coefficients calculated using the above model were multiplied by the irradiance values from the unfiltered simulated solar spectrum in order to demonstrate the relative contributions of different wavelengths of light to inactivation under typical sunlight conditions.

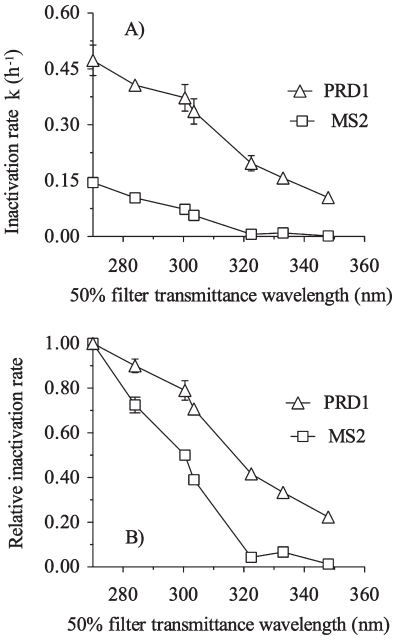

Figure 1. Effect of simulated sunlight wavelength on (A) MS2 and PRD1 inactivation rate constant $k(m^2/MJ)$ and B) k normalized relative to full simulated sunlight ("no filter"). k's from Table 1 were plotted against each of six sunlight filters 50% transmittance values in nm. $k = k_{sun} - k_{dark}$ and was the mean of $n = 3$ trials. Full simulated sunlight was represented at 270 nm at our discretion.

These irradiance-weighted spectral sensitivity coefficients are referred to below as "photodamage coefficients" $(D^i(\lambda) = I_0(\lambda) \times P^i(\lambda))$ for convenience.

Literature Review. Virus action spectra were reviewed from nearly twenty publications since 1934. Two papers[19,20] reported enough data to make direct comparisons with our work, and their data were captured using Graph Grabber software (http://www.quintessa.org/FreeSoftware/GraphGrabber/) and converted to inactivation rate constants (k) with units of m^2/MJ (megajoule).

Statistical Tests. Statistical tests were performed using MATLAB and Prism (GraphPad Software, La Jolla, CA). ANOVA and Tukey's post-test were used to compare virus inactivation rate constants within a single virus type, and two-tailed t tests were used to compare between PRD1 and MS2 rate constants within filter treatments.

RESULTS

Inactivation Rates of MS2 and PRD1. Virus inactivation roughly followed first-order kinetics for each filter condition (SI Figure S2). Within each virus type, there were significant differences among inactivation rate constants for the seven different filter conditions ($p < 0.0001$, ANOVA). However, Tukey's post-test showed that MS2 inactivation rate constants for dark controls were not significantly different from k values for samples irradiated in reactors with f-320, f-335, or f-345 filters (Table 1, SI Figure S2). All other filters produced MS2 inactivation rate constants significantly different from the dark control ($p < 0.05$) and, as expected, filters transmitting increasing amounts of UVB light produced successively (and significantly) faster MS2 inactivation rates (Table 1).

The rate constant for PRD1 dark controls was significantly different from that for each irradiated PRD1 sample ($p < 0.05$)

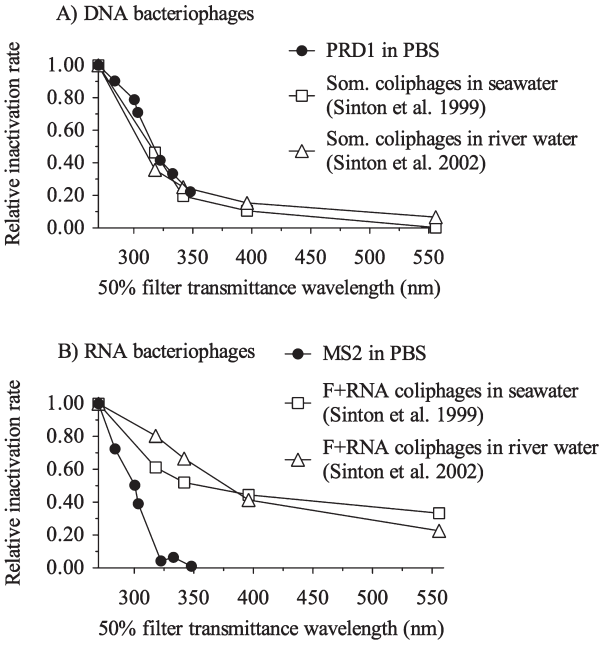

Figure 2. Effect of simulated sunlight wavelength on relative inactivation rate k normalized to full simulated sunlight for (A) DNA bacteriophage and (B) RNA bacteriophage in PBS (circles), seawater (squares), and river water (triangles). $k = k_{sun} - k_{dark}$ and was the mean of $n = 3$ trials for MS2 and PRD1 ($n = 2$ for f-280), and $n = 1$ F+ RNA and somatic coliphage. Inactivation rates for F+ RNA and somatic coliphage from Sinton and colleagues.[19,20]

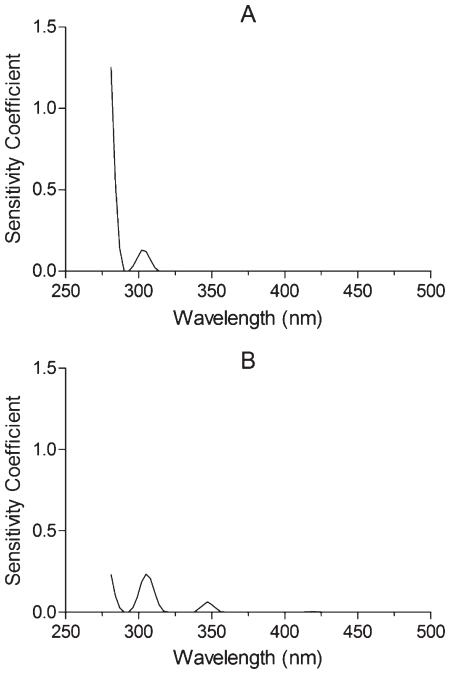

Figure 3. Calculated sensitivity coefficients for (A) MS2 and (B) PRD1 from 280 to 500 nm. Sensitivity coefficients (in $m^2/W \cdot h$) illustrate the contribution of a given irradiance ($W/m^2 \cdot nm$) at each wavelength to the observed inactivation rate (1/h). Each figure represents the single best fit model solution.

(Table 1). No significant difference ($p < 0.05$) in PRD1 inactivation rate constants was observed among f-280, f-295, and f-305 filters, although they were each less effective than no filter at inactivating PRD1. Inactivation rates with the f-335 and f-345 filters were not significantly different from each other. MS2 and PRD1 linear regression R^2 coefficients were high for most samples and were uniformly high for samples with inactivation rates more than two standard deviations above those of the dark controls (Table 1). There was no difference in the inactivation rates of MS2 and PRD1 in the dark controls ($p = 0.7474$, two-tailed t test).

Action Spectra of MS2 and PRD1. The rate of inactivation for both viruses decreased with increasing 50% cutoff filter wavelengths. PRD1 was inactivated faster than MS2 by simulated sunlight under each filter condition tested ($p < 0.05$ for each test, two-tailed t test) (Figure1A). For filters with 50% cutoff wavelengths in the UVB range, PRD1 was inactivated three to six times faster than MS2 (Figure1A). MS2 was not inactivated when filters with 50% cutoff wavelengths in the UVA range were used, while PRD1 was inactivated.

Values of k_{obs} were normalized relative to full simulated sunlight (i.e., no filter treatment) (Figure1B), emphasizing the fact that longer wavelengths contributed more to the inactivation of PRD1 than to that of MS2.

Comparisons to Published Action Spectra. Normalized k_{obs} values for MS2 and PRD1 were compared with extrapolated normalized k_{obs} values from the literature.[19,20] In our solar simulator, PRD1 had a normalized inactivation rate profile similar to the profiles observed for somatic coliphage naturally present in wastewater as extrapolated from the work conducted by Sinton and colleagues in natural sunlight[19,20] (Figure2A). Both PRD1 and somatic coliphage were sensitive to wavelengths in the UVA range.

The relative inactivation rate profiles of F+ RNA coliphage, as extrapolated from the work of Sinton and colleagues,[19,20] were similar to each other and both profiles were different from the profile of MS2 (a type of F+ RNA coliphage) observed in our study using simulated sunlight (Figure 2B). UVB wavelengths were alone responsible for the majority of the MS2 inactivation in our work, while Sinton et al.'s findings showed UVA and visible wavelengths were also important to F+ RNA coliphage inactivation.

Computational Model for MS2 and PRD1 Inactivation. Spectral sensitivity coefficients (see eq 1) for MS2 and PRD1 were determined from the experimentally measured inactivation rate constants using a novel computational approach. Both MS2 and PRD1 were more sensitive to simulated sunlight at 280 nm (the shortest wavelength measured) than to other wavelengths, with sensitivity coefficients decreasing to a local minimum around 290−295 nm (SI Table S1, Figure 3). At longer wavelengths, MS2 and PRD1 had peaks at approximately 305 nm, while PRD1 also exhibited a peak at approximately 350 nm; neither virus was sensitive to visible wavelengths in the PBS solution used for all experiments.

A sensitivity analysis indicated that the peaks in virus sensitivity below 300 nm and at 305−315 nm were robust to random perturbation, as indicated by the prevalence of nonzero values generated by the analysis in these wavelength regions (SI Figure S3 A, B). The third peak observed for PRD1 at approximately 350 nm was less robust, as an alternate model solution was common, in which the second two peaks were merged into a single peak (SI Figure S3 B). This peak is particularly difficult to verify because the optical cutoff filters used did not provide sufficient resolution at these longer wavelengths (SI Figure S8).

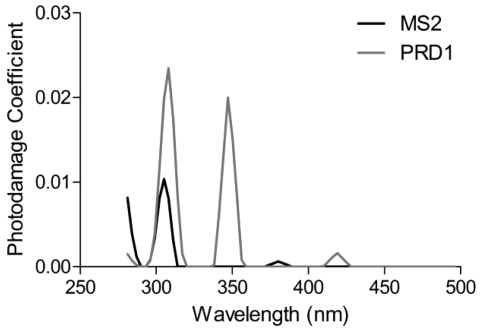

Figure 4. Calculated irradiance-weighted spectral sensitivity coefficients (photodamage coefficients: $D^i(\lambda) = I_0(\lambda) \times P^i(\lambda)$) for (A) MS2 and (B) PRD1 from 280 to 500 nm. Photodamage coefficients (in nm/h) illustrate the contribution of a given wavelength of typical simulated sunlight to the observed inactivation rate (in 1/h). Each figure represents the product of the unfiltered simulated solar irradiance spectrum and the lowest error single solution for the spectral sensitivity coefficients $P(\lambda)$ generated by repeated model runs as presented in Figure 3. The total area under each curve is equal to the inactivation rate constant measured for that organism under the no filter condition (see eq 2).

Single-peak back-tests revealed relatively sound model performance at all wavelengths below 450 nm (SI Figure S4), while three-peak back-testing results demonstrated reasonable accuracy from 285 - 345 nm but not outside of that range (SI Figures S5, S6). The "no-peak" back-test produced reasonably accurate results over the 280−496 nm range and did not produce significant artifactual peaks (SI Figure S7). It was encouraging that neither the sensitivity analysis nor the back-test validation procedures produced large "false peaks" under the conditions tested, although a small false "daughter" peak occurred next to a larger peak in one 3-peak back-test trial (SI Figure S6 C), and some instances of peaks merging (SI Figure S6 D) or being split in two (SI Figure S6 H) occurred at longer wavelengths (>345 nm).

Two additional measures of model robustness, the sum of absolute errors from single peak back-tests and standard deviation of transmittance values among the seven filters were plotted as a function of wavelength (SI Figure S8). Error values were highest above 450 nm with a smaller peak at 290 nm, while transmittance variance was lowest below 300 nm.

Irradiance-weighted photodamage spectra show the relative contributions of different wavelengths of light to inactivation under typical sunlight conditions. From SI Table S2 and Figure 4, it can be seen clearly that the sensitivity of PRD1 to longer wavelengths, which are present in much higher intensity in sunlight, results in an overall higher inactivation rate constant compared to MS2. The small peaks in photodamage coefficients observed at 380 nm for MS2 and approximately 420 nm for PRD1 were not found to be significantly different from the baseline in sensitivity analyses, and are estimated to account for less than 5% of inactivation under typical sunlight conditions. Thus, while it is not known whether these peaks are authentic or artifactual, they are likely to be negligible for most applications.

DISCUSSION

Sensitivity of MS2 and PRD1 to Simulated Sunlight. PRD1 was found to be more sensitive to simulated sunlight than MS2 for all conditions studied, particularly to UVA light, which had little effect on MS2. The greater sensitivity of PRD1 is consistent with that phage's larger genome, and is in agreement with most previous studies,[22,25] although Hotze and colleagues[26] found that MS2 was more sensitive than PRD1 to UVA light from a fluorescent UVA source. This discrepancy is puzzling, but may be due to differences in experimental methods and in the output spectra of the light sources used.

Model-Derived Sensitivity Spectra. Published virus action spectra are typically characterized by peaks around 260 nm where DNA and RNA maximally absorb UV, followed by a steady decline in virus susceptibility up to approximately 300 nm, where most researchers stopped collecting data.[27] We studied inactivation and sensitivity from 280 to 500 nm to explore the effects of all likely biocidal sunlight wavelengths on viruses. While the precise mechanisms of inactivation remain unknown, absorption of UVB and UVA photons by the two basic components of viruses, nucleic acids and proteins, may be a critical step in the inactivation of MS2 and PRD1 in PBS.[27,28] These excited chromophores may undergo direct photolysis or react in aerobic solutions to form reactive oxygen species that damage other targets.[27] A study on the inactivation of MS2 by UVC suggests that nucleic acids may photosensitize damage to proteins;[14] such protein-genome interactions might play a similar role in UVB-mediated damage.

The observation that both MS2 and PRD1 were highly sensitive to the shortest simulated sunlight wavelengths (280−290 nm) is consistent with direct or indirect nucleic acid-sensitized damage. By contrast, the sensitivity peaks identified for both bacteriophages in the 305−310 nm region (Figure3), while similar to a ∼313 nm shoulder in the UV sensitivity of T4 bacteriophage,[18] do not correspond to known peaks for DNA or RNA absorbance or photodamage. These peaks may represent absorbance by and damage to aromatic amino acids (e.g., tryptophan) or other protein components. Light at 254 nm can damage amino acid residues in the protein capsid of MS2[14] and UVB light might produce similar damage, affecting viruses' capsid integrity or their ability to attach to, infect, or replicate within a host. While previous MS2 absorbance spectra did not reveal a peak near 305−310 nm,[29] nor did quantum yield data reveal a peak in that range for many viruses of interest,[27] neither approach measured virus inactivation in the 305−310 nm region. However, circular dichroism (CD) spectroscopy (a technique that measures protein folding and stability under stress) showed aromatic amino acid activity at 305−310 nm for hepatitis C virus.[30] Thus, spectra for photochemical activity and/or virus inactivation may differ from absorbance spectra.[31] Sunlight absorption by and damage to viral nucleic acids and proteins should be measured in parallel with loss of infectivity to further elucidate the mechanisms of inactivation.

The Role of Photosensitizers. We attempted to eliminate all sensitizers from our experimental solutions, whereas Sinton et al.'s work was performed in river water or seawater spiked with 2−3% (v/v) waste stabilization pond effluent or sewage,[19,20] and thus very likely contained significant concentrations of photosensitizers. Our normalized MS2 inactivation rates were far lower than those of Sinton et al.'s F+ RNA coliphage (a family to which MS2 belongs), particularly at longer wavelengths (Figure 2B). Although biological differences may partly explain the variations in spectral response, a more likely explanation is that photons at longer wavelengths were absorbed by photosensitizers in Sinton et al.'s reactors, producing ROS such as singlet oxygen which subsequently damaged the coliphage.[15,32,33] Interestingly, the

normalized inactivation rates of PRD1 in our study were in good agreement with the rates for somatic coliphage reported by Sinton and colleagues (Figure 2A). This agreement may be coincidental, or may indicate similar spectral sensitivity of PRD1 and somatic coliphage to sunlight, and may likewise indicate that exogenous photosensitizers did not play a significant role in the inactivation of the latter variety of somatic coliphages. It should be noted that somatic coliphage are a diverse group, and variable response to sunlight has been documented in field isolates.[22]

Sensitivity Analysis. The results of the sensitivity analysis (SI Figure S3) and model back-testing (SI Figures S4−S8) suggest that the computational model produced reasonable estimates of virus sensitivity to simulated sunlight over the 285−345 nm range, and that the spectral sensitivity peaks observed at wavelengths <300 nm and between 305 and 310 nm are likely to be genuine, although the magnitudes predicted by the model may not be exact. For PRD1, an apparent peak at approximately 350 nm should be interpreted with some caution, as it falls outside the region over which the model could predict with confidence. It cannot be conclusively determined whether PRD1 has two distinct peaks at 305 and 350 nm (as our unperturbed model indicates) or a single, broader peak at slightly longer wavelengths (as the sensitivity analysis suggests). Nonetheless, the inactivation behavior of PRD1 under typical sunlight conditions would be quite similar for both sensitivity spectra.

Future action spectrum experiments with filters providing greater resolution at wavelengths below 285 nm and above 345 nm would increase the power of the current method and its ability to characterize and resolve the sensitivity of viruses over a broader range of sunlight wavelengths. Furthermore, eliminating the atmospheric attenuation filter used in this trial could increase simulated sunlight intensity below 300 nm and increase resolution at the shortest UVB wavelengths.

Advantages and Limitations of the Study Design and the Computational Model. Many action spectra have relied on monochrometers to produce narrow bands of light or simple optical filters to produce sharp cutoffs. When observed biological responses are attributed to the desired spectrum (i.e., the central wavelength of a monochromator slit or the wavelengths above a filter's nominal cutoff), rather than to the entire spectrum transmitted, significant errors may occur. Furthermore, light sources with discrete emission bands such as mercury vapor lamps may introduce artifacts by delivering unrealistically high intensities at wavelengths of low organism sensitivity, while delivering little or no intensity at highly biocidal wavelengths. This study used a xenon arc lamp and optical filters to produce polychromatic light that was similar in intensity and spectral properties to natural sunlight. By taking advantage of the gradual cut-offs of optical filters and by modeling inactivation as a function of actual irradiances reaching target organisms, we were able to resolve detailed viral responses to simulated sunlight wavelengths.

However, additional resolution was obtained at the cost of greater uncertainty. Sensitivity coefficients produced by the model are estimates based on optimizations of an under-determined system, rather than direct measurements. This uncertainty could be reduced by using greater numbers of filters with more diverse transmittance values over the wavelength ranges of interest. Furthermore, higher order terms could be included in future models to address possible synergistic effects between wavelengths. Finally, further work is required to assess the effects of using PBS for inactivation experiments. This buffer contains far more phosphate than natural waters and lacks divalent cations, and may thus affect the speciation of transition metals and the surface charge and aggregation of viruses in photoinactivation trials.

Applications of Action Spectra Findings. Measuring the sensitivity of organisms to polychromatic light is critical for modeling sunlight-mediated inactivation in processes including solar water disinfection, wastewater stabilization pond operation, and the fate of pathogens in recreational waters. In clear waters, eq 2 and the sensitivity coefficients from Figure 3 can be used to estimate MS2 and PRD1 inactivation rate constants for any time of day, season, and latitude for which irradiance spectra can be measured or modeled. Accounting for light attenuation with depth would further allow the impacts of mixing and stratification on sunlight-mediated inactivation to be explored. Similar approaches are widely applied for estimating the photodegradation rates of chemicals in natural waters based on the quantum yield for the transformation of interest;[34,35] the sensitivity coefficients for viruses, $P^i(\lambda)$, are analogous to the product of a wavelength-specific quantum yield and the compound's molar extinction coefficient. An important next step is to determine the sensitivity coefficients for enteric viruses of interest. For example, Adenovirus type 2 and Poliovirus type 3 were recently found to be significantly inactivated only in the presence of UVB wavelengths, suggesting that these viruses may have action spectra more similar to that of MS2 than PRD1.[22]

Further work is required to refine, validate, and apply our experimental approach and computational model. It should be noted that in waters with significant exogenous photosensitizers, additional inactivation mechanisms may occur,[32] and eq 2 does not account for these. Validation under field conditions is also desirable, for example via focused studies similar to those reported by Boehm and colleagues.[36]

■ ASSOCIATED CONTENT

Supporting Information. This section presents all supporting figures and tables referenced in the text as well as detailed descriptions of additional methods and the MATLAB code for the computational model. This material is available free of charge via the Internet at http://pubs.acs.org.

■ AUTHOR INFORMATION

Corresponding Author

*Phone: 510.643.5023; fax: 510.642.7483; e-mail: nelson@ce.berkeley.edu.

Present Addresses

‡Center for a Livable Future, Bloomberg School of Public Health, Johns Hopkins, 615 N. Wolfe Street, W7007 Baltimore, MD 21205-2179.

Author Contributions

†Michael B. Fisher and David C. Love contributed equally to this work.

■ ACKNOWLEDGMENT

This work was supported by an NSF CAREER/PECASE award to K.L.N. (BES-0239144) and by the U.C. Berkeley Blum Center for Developing Economies.

■ REFERENCES

(1) Hollaender, A.; Oliphant, J. The inactivating effect of monochromatic ultraviolet radiation on influenza virus. *J. Bacteriol.* **1944**, *48* (4), 447–454.

(2) Hollaender, A.; Duggar, B. M. Irradiation of plant viruses and of microörganisms with monochromatic light: III. Resistance of the virus of typical tobacco mosaic and *Escherichia coli* to radiation from lambda 3000 to lambda 2250 A. *Proc. Natl. Acad. Sci. U.S.A.* **1936**, *22* (1), 19–24.

(3) Gates, F. Results of irradiating *Staphylococcus aureus* bacteriophage with monochromatic ultraviolet light. *J. Exp. Med.* **1934**, *60* (2), 179–188.

(4) Hollaender, A.; Emmons, C. W. Wavelength dependence of mutation production in the ultraviolet with special emphasis on fungi. *Cold Spring Harbor Symp. Quant. Biol.* **1941**, *9*, 179–186.

(5) Rundel, R. D. Action spectra and estimation of biologically effective UV radiation. *Physiol. Plant.* **1983**, *58*, 380–386.

(6) Cullen, J. J.; Neale, P. J., Biological weighting functions for describing the effects of ultraviolet radiation on aquatic systems. In *Effects of Ozone Depletion on Aquatic Ecosystems*; Haeder, D. P., Ed.; R.G. Landes: Austin, TX, 1996; pp 97−118.

(7) Powell, W.; Setlow, R. The effect of monochromatic ultraviolet radiation on the interfering property of influenza virus. *Virology* **1956**, *2* (3), 337–43.

(8) Hollaender, A.; Emmons, C. Wavelength dependence of mutation production in ultraviolet with special emphasis on fungi. *Cold Spring Harbor Symp. Quant. Biol.* **1941**, *9*, 179–186.

(9) Rivers, T.; Gates, F. Ultraviolet light and vaccinia virus. II. The effect of monochromatic ultraviolet light upon vaccine virus. *J. Exp. Med.* **1928**, *47*, 45–49.

(10) Stadler, L. J.; Uber, F. M. Genetic effects of ultraviolet radiation in maize. IV. Comparison of monochromatic radiations. *Genetics* **1942**, *27* (1), 84–118.

(11) Jagger, J., Solar-UV actions on living cells. 1985.

(12) Coohill, T. Action spectra again? *Photochem. Photobiol.* **1991**, *54* (5), 859–870.

(13) Eischeid, A. C.; Meyer, J. N.; Linden, K. G. UV disinfection of adenoviruses: Molecular indications of DNA damage efficiency. *Appl. Environ. Microbiol.* **2009**, *75* (1), 23–28.

(14) Wigginton, K. R.; Menin, L.; Montoya, J. P.; Kohn, T. Oxidation of virus proteins during UV254 and singlet oxygen mediated inactivation. *Environ. Sci. Technol.* **2010**, *44* (14), 5437–5443.

(15) Kohn, T.; Nelson, K. L. Sunlight-mediated inactivation of MS2 coliphage via exogenous singlet oxygen produced by sensitizers in natural waters. *Environ. Sci. Technol.* **2007**, *41* (1), 192–7.

(16) Peak, M. J.; Peak, J. G. Action spectra for the ultraviolet and visible light inactivation of phage T7: Effect of host-cell reactivation. *Radiat. Res.* **1978**, *76* (2), 325–30.

(17) Rontó, G.; Gáspár, S.; Bérces, A. Phage T7 in biological UV dose measurement. *J Photochem. Photobiol. B, Biol.* **1992**, *12* (3), 285–94.

(18) Tyrrell, R. M. Solar dosimetry with repair deficient bacterial spores: action spectra, photoproduct measurements and a comparison with other biological systems. *Photochem. Photobiol.* **1978**, *27* (5), 571–9.

(19) Sinton, L.; Hall, C.; Lynch, P.; Davies-Colley, R. Sunlight inactivation of fecal indicator bacteria and bacteriophages from waste stabilization pond effluent in fresh and saline waters. *Appl. Environ. Microbiol.* **2002**, *68* (3), 1122–1131.

(20) Sinton, L. W.; Finlay, R. K.; Lynch, P. A. Sunlight inactivation of fecal bacteriophages and bacteria in sewage-polluted seawater. *Appl. Environ. Microbiol.* **1999**, *65* (8), 3605–13.

(21) *Method 1601: Male-Specific (F+) and Somatic Coliphage in Water by Two-Step Enrichment Procedure*, 821-R-01-030; U.S. Environmental Protection Agency: Washington, DC, . 2001; p 25.

(22) Love, D. C. S.; Andrea, C.; Nelson, Kara L. Human virus and bacteriophage inactivation in clear water by simulated sunlight compared to bacteriophage inactivation at a southern California beach. *Environ. Sci. Technol.* **2010**, *44* (18), 6965–6970.

(23) Adams, M. H., *Bacteriophages*; Interscience Publishers: New York, 1959.

(24) Bolton, J. R.; Linden, K. G. Standardization of methods for fluence (UV dose) determination in bench-scale UV experiments. *J. Environ. Eng.* **2003**, *129* (3), 209–216.

(25) Lytle, C. D.; Sagripanti, J. L. Predicted inactivation of viruses of relevance to biodefense by solar radiation. *J. Virol.* **2005**, *79* (22), 14244–52.

(26) Hotze, E. M.; Badireddy, A. R.; Chellam, S.; Wiesner, M. R. Mechanisms of bacteriophage inactivation via singlet oxygen generation in UV illuminated fullerol suspensions. *Environ. Sci. Technol.* **2009**, *43* (17), 6639–45.

(27) Rauth, A. The physical state of viral nucleic acid and the sensitivity of viruses to ultraviolet light. *Biophys. J.* **1965**, *5*, 257–273.

(28) Chen, R. Z.; Craik, S. A.; Bolton, J. R. Comparison of the action spectra and relative DNA absorption spectra of microorganisms: Information important for the determination of germicidal fluence (UV dose) in an ultraviolet disinfection of water. *Water Res.* **2009**, *43*, 5087–5096.

(29) Johnson, H. R.; Hooker, J. M.; Francis, M. B.; Clark, D. S. Solubilization and stabilization of bacteriophage MS2 in organic solvents. *Biotechnol. Bioeng.* **2007**, *97* (2), 224–34.

(30) Kunkel, M.; Watowich, S. J. Biophysical characterization of hepatitis C virus core protein: Implications for interactions within the virus and host. *FEBS Lett.* **2004**, *557* (1−3), 174–80.

(31) Chen, R. Z.; Craik, S. A.; Bolton, J. R. Comparison of the action spectra and relative DNA absorbance spectra of microorganisms: Information important for the determination of germicidal fluence (UV dose) in an ultraviolet disinfection of water. *Water Res.* **2009**, *43* (20), 5087–5096.

(32) Kohn, T.; Grandbois, M.; McNeill, K.; Nelson, K. L. Association with natural organic matter enhances the sunlight-mediated inactivation of MS2 coliphage by singlet oxygen. *Environ. Sci. Technol.* **2007**, *41* (13), 4626–4632.

(33) Davies-Colley, R. J.; Donnison, A. M.; Speed, D. J.; Ross, C. M.; Nagels, J. W. Inactivation of faecal indicator microorganisms in waste stabilisation ponds: Interactions of environmental factors with sunlight. *Water Res.* **1999**, *33* (5), 1220–1230.

(34) Schwartzenbach, R. P. G., P.M.; Imboden, D. M., *Environmental Organic Chemistry*, 2nd ed.; John Wiley and Sons: Hoboken, NJ, 2003.

(35) Zepp, R. G.; Cline, D. M. Rates of direct photolysis in aquatic environment. *Environ. Sci. Technol.* **1977**, *11* (4), 359–366.

(36) Boehm, A. B.; Yamahara, K. M.; Love, D. C.; Peterson, B. M.; McNeill, K.; Nelson, K. L. Covariation and photoinactivation of traditional and novel indicator organisms and human viruses at a sewage-impacted marine beach. *Environ. Sci. Technol.* **2009**, *43* (21), 8046–52.